A TRANSIENT FINITE ELEMENT ANALYSIS OF UNSTABLE CRACK PROPAGATION IN SOME 2-DIMENSIONAL GEOMETRIES

P. N. R. Keegstra*, J. L. Head** and C. E. Turner***

INTRODUCTION

Analytical solutions have been obtained to the problem of unstable crack propagation in an infinite plate by Freund [1] and in an infinite strip by Nilsson et al [2, 3, 4]. An extensive review of this work has been presented by Erdogan [5]. Recently, interest has extended to the problem of the analysis of crack propagation and arrest in finite geometries. There is interest in the analysis for standard 2-dimensional test piece geometries for which dynamic toughness data are known with some confidence. Also, there is interest in the modelling of crack propagation in real components, having more complex 2-dimensional, or, eventually, 3-dimensional geometries and for which the relevent toughness data are known. This paper describes, in outline, a 2-dimensional dynamic linear elastic finite element programme, based on triangular linear displacement plane strain elements, suitable for either purpose. Applications described here are restricted to test piece geometries.

It was thought convenient to use double cantilever beam (DCB) geometries, under fixed grip loading conditions, for the validation of the programme. For this geometry, there is a large volume of experimental data, assembled by Hahn et al [6, 7, 8]. The present paper gives the results of analyses for DCB geometry and a comparison with the published experimental results of Hahn et al. The paper also describes the application of the programme to finite strip geometries, also under fixed grip conditions. In conventional tests on metals, the problem is circuitous. Without a dynamic analysis of the test piece, the dynamic toughness (which is, in general, a function of crack speed) cannot be derived. On the other hand, the programme can be run only if the dynamic toughness data are input. The dynamic toughness can be measured however, without the use of a dynamic stress analysis, by the thermal wave technique [9], dynamic photoelasticity [10] or the shadow optical method [11].

The dynamic energy release rate, G_D, in a specimen under fixed-grip conditions, is [5]

$$G_D = - \left(\frac{dU}{da} + \frac{dS}{da} \right) \qquad (1)$$

where S = kinetic energy

* Royal Netherlands Navy, seconded to Imperial College, London, England.
** Department of Mechanical Engineering, Imperial College of Science and Technology, Exhibition Road, London, SW7 2BX, London, England.
***Imperial College, London, seconded to National Physical Laboratory, Teddington, England.

(other symbols conform to the standard nomenclature list.) In the analyses described in the paper, it was assumed that energy is dissipated only at the crack front. There may be damping losses, either internally and/or at boundaries. The inclusion of these losses in the analysis would, in principle, present no difficulty, although the assessment of a reasonable magnitude would not be easy. The nature of energy dissipation at the crack front is not discussed in the paper, but dissipation is, by implication, taken into account by use of a generalised surface energy of the Irwin-Orowan type. The method by which this is included in the analysis is described in the paper. The energy balance equation is then

$$G_D = R(v) \tag{2}$$

where $R(v)$ = dynamic fracture toughness, which in general is a function of the crack speed v.

DYNAMIC ANALYSIS

The finite element discretisation of a continuum leads to the well-known matrix form of the equation of motion [12].

$$\underline{K}\,\underline{u} + \underline{C}\,\dot{\underline{u}} + \underline{M}\,\ddot{\underline{u}} = F(t) \tag{3}$$

where
$\underline{K}$ = stiffness matrix
$\underline{C}$ = viscosity matrix
$\underline{M}$ = mass matrix
$\underline{u}$ = displacement vector
$\underline{F}(t)$ = force vector

and the dot indicates the derivative with respect to time. In the analyses described in the paper, the mass of each element was assumed to be concentrated at the nodes, thus diagonalising the mass matrix and reducing the computing time by up to 80% with an acceptable loss of accuracy (about 4%). Equation (3) is integrated stepwise in time in a manner similar to that described by Hitchins and Dance [13]. A second order Lagrangian polynomial is assumed to relate the accelerations at sequential time points, thus the displacements and velocities at time $t + \Delta$ are related to those at t and $t - \Delta$ by the following equation (see Keegstra [14]).

$$\begin{Bmatrix} \underline{u}_+ \\ \dot{\underline{u}}_+ \end{Bmatrix} = \begin{bmatrix} \underline{I} & \Delta\underline{I} \\ \underline{0} & \underline{I} \end{bmatrix} \begin{Bmatrix} \underline{u}_o \\ \dot{\underline{u}}_o \end{Bmatrix} + \begin{bmatrix} -\frac{\Delta^2}{24}\underline{I} & \frac{5\Delta^2}{12}\underline{I} & \frac{\Delta^2}{8}\underline{I} \\ -\frac{\Delta}{12}\underline{I} & \frac{2\Delta}{3}\underline{I} & \frac{5\Delta}{12}\underline{I} \end{bmatrix} \begin{Bmatrix} \ddot{\underline{u}}_- \\ \ddot{\underline{u}}_o \\ \ddot{\underline{u}}_+ \end{Bmatrix} \tag{4}$$

The subscripts +,o,- denote the values at times $t + \Delta$, t, $t - \Delta$ respectively. $\underline{I}$ denotes unit matrix and Δ is the time interval. The predicted accelerations $\ddot{\underline{u}}_+$ are used with equation (4) to obtain a first estimate of the velocities $\dot{\underline{u}}_+$ and displacements $\underline{u}_+$, which are then substituted

into equation (3) to obtain improved values of the accelerations $\ddot{\underline{u}}_+$. The iteration is continued until adequate convergence is obtained. The solution is then advanced by a further time step. The length of the time step is taken to be

$$\Delta \leq s/5C_L \tag{5}$$

where
s = smallest finite element side length
C_L = speed of dilatational wave

CRACK EXTENSION CRITERION

At the present stage of the development of the programme, the crack path must be known. In DCB and strip geometries, the crack path may reasonably be assumed to be the plane of symmetry and only one half of the specimen is modelled. Figure 1 shows the DCB geometry for which the present analyses were made. The finite element mesh comprised 250 elements and 157 nodes. Nodes on the plane of symmetry are restrained against displacement normal to the crack plane until the crack front has passed, after which they are released. The forces on the restrained nodes are monitored.

It has been shown by Keegstra [14] that, for a given mesh, the force on the crack tip node is proportional to the stress intensity factor K and may, therefore, be used as a crack extension criterion. In the execution of the programme, the crack tip node is released when the restraining force reaches a prescribed value F_c, which depends on the mesh size and on the dynamic toughness K_D. The crack speed is calculated from the intervals between the release times of adjacent nodes. The crack is assumed to have arrested if the force on the crack tip nodes does not reach F_c within a reasonable period measured from the time at which the previous node is released. This time period is chosen, arbitrarily, to correspond to a crack speed of 0.01 C_L.

When the force on the crack tip node reaches F_c and the node is released, the force is not reduced instantaneously to zero but is reduced linearly with nodal displacement, according to the equation.

$$F_b = F_c(1 - \bar{u}/u_c) \tag{6}$$

where

$$\bar{u} = \int_o^{t^*} \frac{u(t)}{t}\,dt \tag{7}$$

and
u_c = reference displacement
$u(t)$ = nodal displacement
t^* = current time

Thus $\bar{u}$ is a time-averaged displacement. The node therefore does work against the "holding-back" force F_b. This provides an energy sink which, by making an appropriate choice of the reference displacement u_c, represents the generalised surface energy. It has been shown [14] that the appropriate value of u_c is given by

$$u_c = F_c/K_n \quad (8)$$

where K_n is the stiffness of the node. This method of providing an energy sink is illustrated in Figure 2.

DCB ANALYSES

A force was applied to the node representing the loading pin, such that the initial stress intensity factor K_Q reached a value which exceeded K_{1C} by a factor chosen to characterise the bluntness of the initial crack. The dynamic calculation was initiated by releasing the crack tip node. Throughout the analysis, the displacement of the loading pin was held constant, equal to the initial value, modelling fixed-grip conditions.

To enable a comparison with the experimental results of Kobayashi and Mall (see [7]) and the analytical results of Hahn et al [7], the material properties used by those authors, which relate to Homalite-100, were used in the present analyses. Also, the same value of K_Q was used, although this was necessarily inferred from the quoted value of the initial strain energy. Figure 3 shows the assumed relationship between K_D/K_{1C} and crack speed v [7]. Figure 4 shows the relationship between the computed crack speed and crack length. For comparison, the figure also shows the analytical results of Hahn et al and the experimental results of Kobayashi and Mall. Figure 5 shows the variation with time and/or crack length of the various energy terms including the potential energy of the loading pin.

FINITE STRIP ANALYSES

The geometry for which these analyses were made is shown in Figure 6. The specimen was assumed to be of steel. As for the DCB analyses, fixed grip loading conditions were assumed. In each of these analyses, however, the crack tip nodes were released at prescribed time intervals, regardless of the magnitude of the force on the node. In other words, the specimens were assumed to be "sliced" at constant speed. The act of slicing at a given speed implies a certain ratio of static and dynamic energy release rates (G_{STAT}/G_D). The analyses covered a range of constant slicing speeds from 0.18 C_R to 1.8 C_R where C_R is the Rayleigh wave speed. Figure 7 shows the crack face displacement profile at a sequence of time values, for a single slicing speed (2917 m/s = 0.98 C_R). From the figure it may be seen that, for this slicing speed, the crack front propagates at a speed which is lower than the slicing speed. For slicing speeds below about 0.7 C_R, the crack front speed was found to be equal to the slicing speed. For slicing speeds above this value, the crack front speed was always lower than the slicing speed and approached assymptotically the Rayleigh wave speed as the slicing speed was increased. The relationship between the crack front speed and the slicing speed is shown in Figure 8.

For each value of slicing speed, G_D was calculated (using equation (1)) for a sequence of values of crack length. For this geometry, these values were nearly constant over the range of crack length. An average value of G_D was calculated for each slicing speed. The ratio $g(v) = G_D/G_{STAT}$ is shown plotted against the ratio v/C_R in Figure 9. The figure shows the analytical results of Nilsson [2] for an infinite strip. The figure also shows results of similar slicing runs on the DCB geometry shown in Figure 1 and the analytical results of Freund [1] for an infinite plate.

DISCUSSION AND CONCLUSIONS

The close agreement between the predicted and measured crack speeds in the DCB geometry, see Figure 4, gives some confidence in the validity of the computer programme and in the method of modelling the energy sink at the crack tip. Further evidence of the validity of the programme is provided by Figure 3, which shows, in addition to the input relationship between K_D/K_{1C} and v, values of K_D/K_{1C} obtained from the output values of G using the relationship

$$G_D = K_D^2 f(v)/E \quad (9)$$

The function f(v), given by Nilsson [2], depends on the crack speed, shear wave speed, longitudinal wave speed and Poisson's ratio.

The potential energy of the loading pin, shown in Figure 5, exhibits fluctuations which are due to the arrival of stress waves at the loading pin. The propagation of stress waves, and reflections from the boundaries of the specimen, are clearly seen in various forms of graphical output which have been generated, also in a film which has been made from these outputs.

For the finite strip, Figure 9 shows the marked dependence of g(v) on the geometry of the strip. Additional results, obtained for longer strips, show that, as the strip length is increased, g(v) approaches Nilsson's result for an infinite strip. For the finite strip geometry, instantaneous values of G_D never exceeded G_{STAT} by more than a few percent. (Recall that Figure 9 shows the *average* value of g(v) for each crack speed). By contrast, in the DCB geometry, instantaneous values of G_D exceeded G_{STAT} by up to 50%. In other words, in a DCB specimen under fixed grip loading, kinetic energy plays a greater role in the mechanics of crack propagation.

The form of Figure 8 is not yet fully understood by the authors. One possible explanation of the non-linearity, for crack speeds above about 0.7 C_R, is the compressive stress which according to Baker [15] develops ahead of the crack at high crack speeds. Some evidence of this compressive stress was seen in the computer outputs, despite the coarse meshes which were necessarily used.

In conclusion, the results so far obtained give confidence in the validity of the programme. The results presented in the paper provide additional knowledge and understanding of crack propagation in DCB and finite strip geometries. The programme is now being used in the analysis of experimental results for these and other geometries.

REFERENCES

1. FREUND, L. B., J. Mech. Phys. Solids, 20, 1972, 129 and 141.
2. NILSSON, F., Royal Inst. of Tech., Stockholm, Report 8, 1975.
3. CARLSON, J., DAHLBERG, L. and NILSSON, F., Proc. Int. Conf. Dyn. Crack Prop. (ed. Sih, G. C.), 1972.
4. NILSSON, F., Eng. Fract. Mech., 6, 1974, 397.
5. ERDOGAN, "Fracture", (ed. H. Leibowitz), 2, 1968.
6. HAHN, G. T. et al, Battelle Report, BMI 1937, 1975.
7. HAHN, G. T. et al, Battelle Report, BMI 1959, 1976.
8. HAHN, G. T. et al, ASTM STP 601, 1976, 209.

9. WELLS, A. A., Welding Research, 7, 1953, 34.
10. KOBAYASHI, A. S. and MALL, S., Proc. Conf. Dyn. Fract. Toughness, London, 1976, 259.
11. KALTHOFF, J. F. et al, Proc. Symp. Fast Fracture and Crack Arrest, Chicago, 1976.
12. ZIENKIEWICZ, O. C., "The Finite Element Method", McGraw-Hill, London, 1971.
13. HITCHINS, D. and DANCE, S. H., J. Nucl. Eng. and Design, 29, 1974, 311.
14. KEEGSTRA, P. N. R., J. Inst. Nucl. Eng., 17, 89.
15. BAKER, B. R., J. Appl. Mech., 1962, 449.

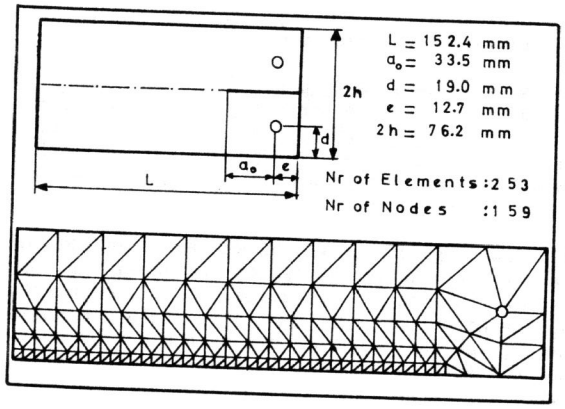

Figure 1 DCB Geometry and Mesh

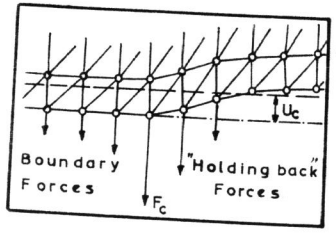

Figure 2 Fracture Energy Model

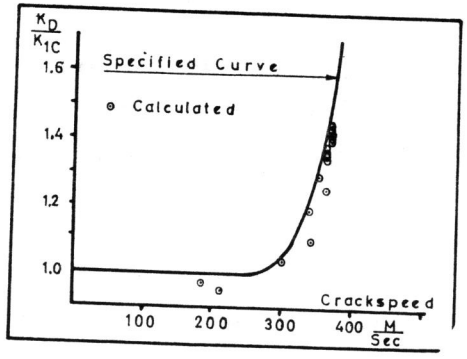

Figure 3 Assumed Relationship Be K_D and Crack Speed (M

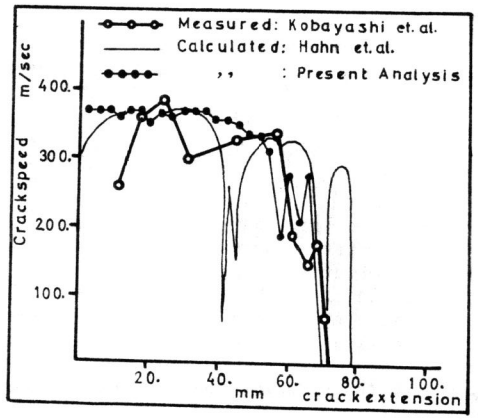

Figure 4 Calculated and Experimental Crack Speed Against Crack Length (DCB)

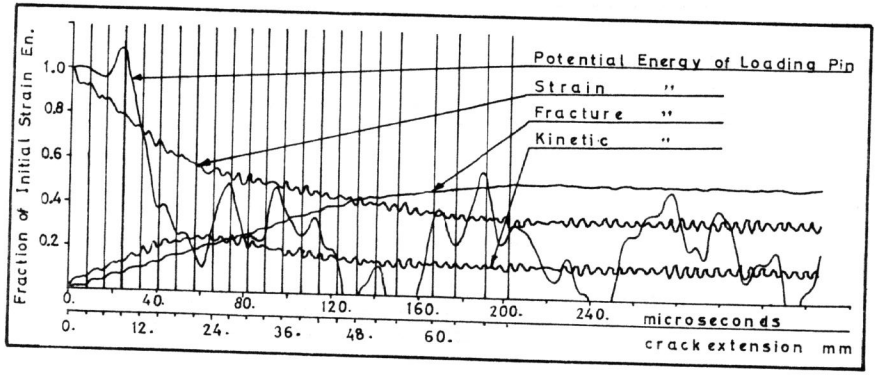

Figure 5 Calculated Energies Against Time and Crack Length (DCB)

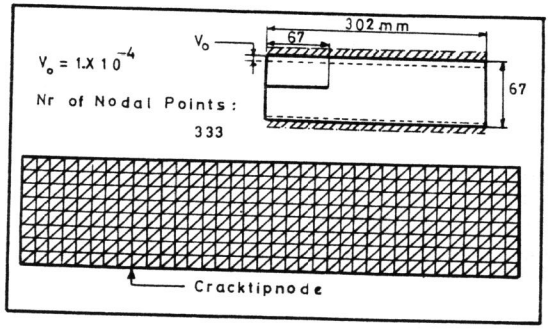

Figure 6 Finite Strip Geometry and Mesh

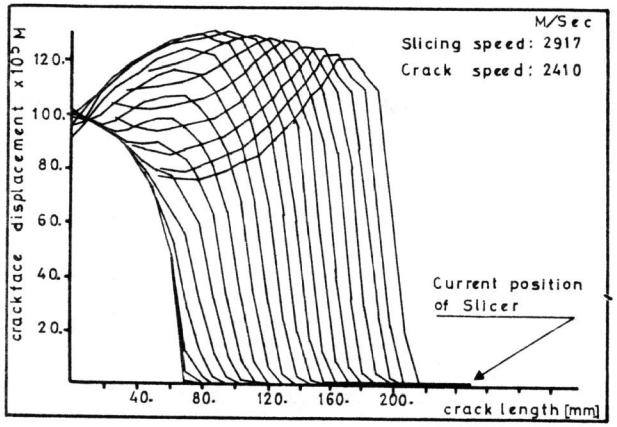

Figure 7 Crack Face Profiles (Finite Strip)

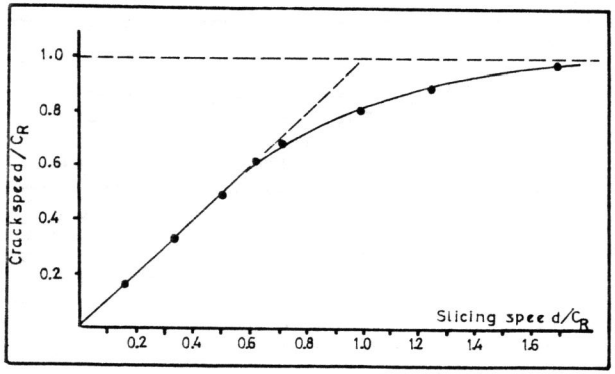

Figure 8 Crack Speed Against Slicing Speed (DCB and Finite Strip)

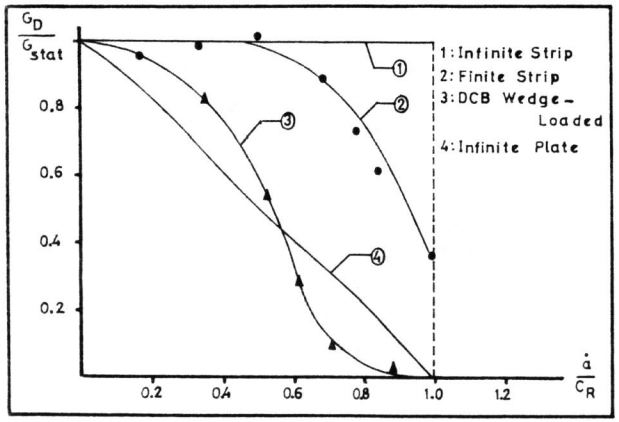

Figure 9 Ratios G_D/G_{STAT} Against Crack Speed